Available online at www.sciencedirect.com
ScienceDirect
Catalysis Today 126 (2007) 290–295
CATALYSIS TODAY
www.elsevier.com/locate/cattod

An investigation of NO/CO reaction over perovskite-type oxide $La_{0.8}Ce_{0.2}B_{0.4}Mn_{0.6}O_3$ (B = Cu or Ag) catalysts synthesized by reverse microemulsion

Hong He *, Mei Liu, Hongxing Dai, Wenge Qiu, Xuehong Zi

Department of Chemistry and Chemical Engineering, College of Environmental and Energy Engineering, Beijing University of Technology, Beijing 100022, China

Abstract

The perovskite-type oxides $La_{0.8}Ce_{0.2}Cu_{0.4}Mn_{0.6}O_3$ and $La_{0.8}Ce_{0.2}Ag_{0.4}Mn_{0.6}O_3$ prepared by reverse microemulsion and sol–gel methods (denoted as R and S, respectively), have been investigated on their catalytic performance for the (NO + CO) reaction, and characterized by means of temperature-programmed desorption (TPD), X-ray diffraction (XRD), transmission electron microscopy (TEM), and X-ray photoelectron spectroscopy (XPS). XRD measurements proved the presence of the perovskite phase with a considerable amount of CeO_2 phase and the formation of CeO_2 phase was restrained with the reverse microemulsion method. TEM investigations revealed that the $La_{0.8}Ce_{0.2}Cu_{0.4}Mn_{0.6}O_3$-R nanoparticles were uniform spheres in shape with diameters ranging from 40 to 50 nm, whereas an aggregation of particles was found for the $La_{0.8}Ce_{0.2}Cu_{0.4}Mn_{0.6}O_3$-S catalyst. The activity of NO reduction with CO decreased in the order of $La_{0.8}Ce_{0.2}Cu_{0.4}Mn_{0.6}O_3$-R > $La_{0.8}Ce_{0.2}Cu_{0.4}Mn_{0.6}O_3$-S > $La_{0.8}Ce_{0.2}Ag_{0.4}Mn_{0.6}O_3$-R > $La_{0.8}Ce_{0.2}Ag_{0.4}Mn_{0.6}O_3$-S. In NO-TPD experiments, the principal desorbed species detected in the effluent was NO with a trace amount of O_2 and N_2O, suggesting that the non-dissociated adsorption of NO on the surface of the perovskite-type oxides was dominant. The XPS results revealed that Ce^{4+} and Cu^{+} was the predominant oxidation state for Ce and Cu components in $La_{0.8}Ce_{0.2}Cu_{0.4}Mn_{0.6}O_3$ and $La_{0.8}Ce_{0.2}Ag_{0.4}Mn_{0.6}O_3$ catalysts. The existence of Cu^{+} ions and its redox reaction ($Cu^{+} \leftrightarrow Cu^{2+}$) would benefit the NO adsorption and reduction by CO.

Keywords: Perovskite-type oxides; NO reduction; Reverse microemulsion

1. Introduction

The reaction of NO and CO has been paid a great attention by many research groups due to its existence in exhaust gases of both mobile and immobile sources. The catalysts employed in the reaction are usually noble metals and perovskite-type oxides. Generally speaking, perovskite-type oxides do not show as good catalytic performance as noble metals. Nevertheless, they have comparable activity and been considered as potential depolluting catalysts in some cases [1].

The physicochemical properties of perovskite-type oxides (general formula ABO_3) can be regulated to meet the requirements of certain desired reactions by partially substituting A and/or B with other metals of different oxidation states since the oxidation state of B cation and the structural defect (such as anionic or cationic vacancies) can be changed by the manipulation. During the past years, the perovskite-type oxides such as $LaMO_3$, $La_{1-x}Sr_xMO_3$ (M = Fe, Co, Mn, Cr, Ni) [2,3], $LaMnO_3$, $LaMn_{0.99}Pt_{0.01}O_3$ [4], $La_{1-x}Sr_xAl_{1-2y}Cu_yRu_yO_3$ [5,6], $LaCoO_3$ [7,8], $La_{0.8}Sr_{0.2}Co_{1-2y}Cu_yRu_yO_3$ [9], $La_{1-x}Sr_x$-FeO_3 [10,11], $La_2Cu_{1-x}Fe_xO_4$[12], and $La_{1-x-y}Sr_xCe_yFeO_3$ [13,14] have been intensively studied and used to catalyze the reaction of NO and CO.

Although perovskite-type catalysts have showed good performance in many reactions, the low surface area is always the disadvantage. Usually, perovskite-type oxides are prepared by calcination at high temperatures (>800 °C), resulting in a surface area of less than 10 $m^2\ g^{-1}$. In order to increase catalytic activity, various attempts to enhance the surface area have been made by using methods such as mist-drying, chelating and metal–citric–cellulose complexing, sol–gel process, and hydrothermal synthesis [15]. Recently, the reverse microemulsion

* Corresponding author. Tel.: +86 10 67396588; fax: +86 10 67391983.
E-mail address: hehong@bjut.edu.cn (H. He).

0920-5861/$ – see front matter © 2007 Published by Elsevier B.V.
doi:10.1016/j.cattod.2007.06.004

technology has been investigated for preparing nanoparticles of pure metal, metal oxides as well as perovskite-type oxides. Giannakas et al. [16] reported that $LaMnO_3$ prepared via cetyltrimethyl ammonium bromide (CTAB)–butanol–octane–nitrate salt microemulsions possessed relatively high specific surface area of 20 $m^2\ g^{-1}$ and nanoparticle size of 20–100 nm, which was claimed to be a promising catalyst as a substitute for noble metals in the de-NO_x application.

In this work, the perovskite-type oxides $La_{0.8}Ce_{0.2}Cu_{0.4}Mn_{0.6}O_3$ and $La_{0.8}Ce_{0.2}Ag_{0.4}Mn_{0.6}O_3$ were prepared by reverse microemulsion and sol–gel methods. The performance of the two kinds of perovskite-type oxides for the reaction of NO and CO and the characterization of the materials using temperature-programmed desorption (TPD), X-ray diffraction (XRD), transmission electron microscopy (TEM), and X-ray photoelectron spectroscopy (XPS) are reported.

2. Experimental

2.1. The preparation of $La_{0.8}Ce_{0.2}Cu_{0.4}Mn_{0.6}O_3$-S and $La_{0.8}Ce_{0.2}Ag_{0.4}Mn_{0.6}O_3$-S

The $La_{0.8}Ce_{0.2}Cu_{0.4}Mn_{0.6}O_3$-S and $La_{0.8}Ce_{0.2}Ag_{0.4}Mn_{0.6}O_3$-S catalysts were prepared by means of citric acid complexing sol–gel process [17]. $La(NO_3)_3{\cdot}6H_2O$ (Beijing Chemical Reagents Company, >99%), $Ce(NO_3)_3{\cdot}6H_2O$ (Beijing Chemical Reagents Company, >99%), $Cu(NO_3)_2{\cdot}3H_2O$ (Sinopharm Group Chemical Rengent Co, >99.5%) or $AgNO_3$ (Beijing Chemical Reagents Company, >99.8%), and $Mn(NO_3)_2$ hydrosolution (Beijing Yili Fine Chemical Reagents Company, >49%) at the appropriate ratio were mixed in aqueous solution. Citric acid (Aldrich, >99%) equimolar to the metals was added. The solution was then evaporated at 80 °C to produce a viscous syrup. After subsequent evaporation at 120 °C for 8 h and calcination at 850 °C in air for 10 h, the material was in turn ground, tabletted, crushed, and sieved to a size range of 60–80 mesh.

2.2. The preparation of $La_{0.8}Ce_{0.2}Cu_{0.4}Mn_{0.6}O_3$-R and $La_{0.8}Ce_{0.2}Ag_{0.4}Mn_{0.6}O_3$-R

Two reverse microemulsions of CTAB/1-butanol/water/*n*-heptane with identical weight ratios of CTAB:1-butanol:water:*n*-heptane = 21:15:27:37 were prepared: one comprising desired amounts of chemicals same as those used in Section 2.1 (denoted as precursor solution A), the other comprising a precipitating agent of 0.5 M NaOH solution (denoted as precursor solution B). Equal amounts of the two precursor solutions A and B were mixed together with continuous stirring at 30 °C for 2 h. After the particles were formed in water droplets, they were not precipitated and the mixed microemulsion containing the particles remained transparent due to the adsorption of surfactant molecules at the oil/water interface. After acetone was added, the reaction occurred and the result was the destruction of the microemulsion and the generation of co-precipitation. Then, the as-received precipitations were washed with acetone and water repeatedly to remove the oil, remained Na^+, and surfactant molecules adsorbed on the surfaces of particles. Finally, the washed particles were collected, dried at 120 °C for 8 h and calcined at 850 °C in air for 10 h. The obtained powders were in turn ground, tabletted, crushed, and sieved to a size range of 60–80 mesh.

2.3. Reaction and characterization

The catalytic activity of NO and CO reaction was evaluated in a quartz tube micro-reactor (i.d. = 10 mm) with a gas mixture of 1%NO + 1%CO + 98% He. The space velocity (SV) was 20,000 h^{-1}. Five hundred milligrams of the catalyst was packed in the middle of the reactor between two plugs of quartz. A thermocouple was placed in direct contact with the catalyst for accurate temperature measurement. Products were analyzed, usually 30 min after temperature stabilization, by an on-line gas chromatograph (Shimadzu GC-14C). A Porapak Q + R column, which was dipped in a acetone-water-$CaCl_2{\cdot}6H_2O$ bath to keep the column temperature of −20 °C, was used to separate NO, NO_2, and N_2O. A 5A molecular sieve column was used (in parallel) to separate N_2, O_2, CO, and CO_2.

The NO-TPD experiments were carried out in a similar micro-reactor. Before performing a TPD experiment, the samples (50 mg) were heated to 800 °C in O_2 and maintained at the temperature for 1 h in order to clean the surface of the samples and then pretreated in situ in NO (30 ml min^{-1}) at 450 °C for 1 h, followed by cooling to room temperature in the same atmosphere and purging with He for 10 min. After being cooled to room temperature, the sample was heated from 30 to 850 °C at a rate of 15 °C min^{-1}. The effluent gases were monitored and analyzed on-line by a mass spectrometer (Hiden, HPR20).

The crystal structures of the catalysts were determined by an X-ray diffractometer (D8 Advance) operating at 35 kV and 35 mA using Cu Kα radiation. The patterns recorded were referred to the powder diffraction files—1998 ICDD PDF database for the identification. The specific surface areas of catalysts were measured using the BET method on an ASAP2020 apparatus.

XPS (Leybold Heraeus-Shenyang SKL-12) technique was used to determine the core-level binding energies of the cations in the catalysts, using monochromatic Al Kα as the excitation source. Before carrying out the XPS experiments, the samples were treated in O_2 (30 ml min^{-1}) at 800 °C for 1 h. The C 1s line at 284.6 eV was taken as a reference for binding energy calibration.

3. Results

3.1. Catalytic performance for the (NO + CO) reaction

The catalytic performance of the four catalysts for the (NO + CO) reaction at SV = 20,000 h^{-1} is shown in Figs. 1 and 2. Only N_2, N_2O, and CO_2 were detected in the reaction effluents under the adopted reaction conditions. Over all the catalysts investigated in the present work, the NO conversion increased with the rise in temperature. From Fig. 2, one can see that the N_2O yield increased at first and then decreased with

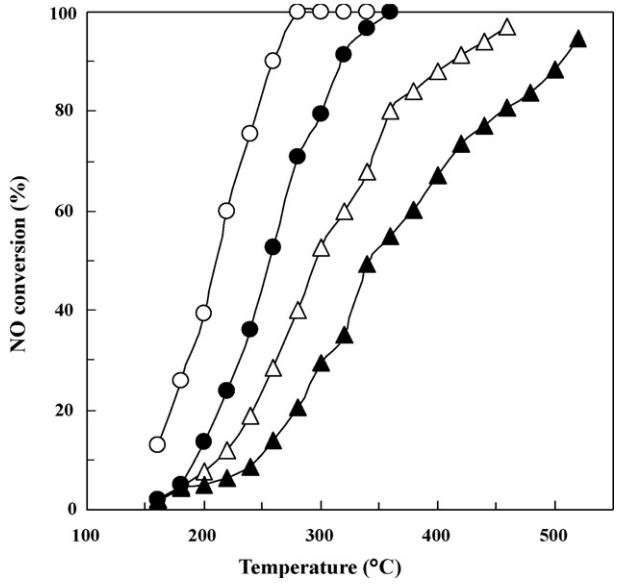

Fig. 1. NO conversion over (○) $La_{0.8}Ce_{0.2}Cu_{0.4}Mn_{0.6}O_3$-R, (●) $La_{0.8}Ce_{0.2}Cu_{0.4}Mn_{0.6}O_3$–S, (△) $La_{0.8}Ce_{0.2}Ag_{0.4}Mn_{0.6}O_3$-R, and (▲) $La_{0.8}Ce_{0.2}Ag_{0.4}Mn_{0.6}O_3$-S catalysts for the reaction of NO and CO at SV = 20,000 h^{-1}.

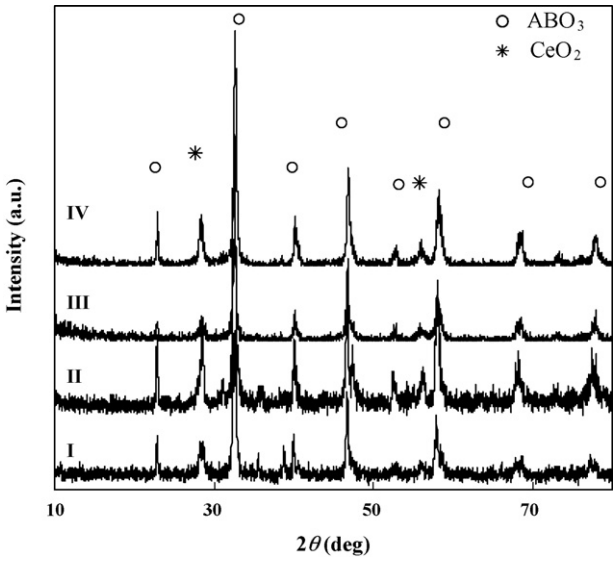

Fig. 3. XRD profiles of (I) $La_{0.8}Ce_{0.2}Cu_{0.4}Mn_{0.6}O_3$-R, (II) $La_{0.8}Ce_{0.2}Cu_{0.4}Mn_{0.6}O_3$-S, (III) $La_{0.8}Ce_{0.2}Ag_{0.4}Mn_{0.6}O_3$-R, and (IV) $La_{0.8}Ce_{0.2}Ag_{0.4}Mn_{0.6}O_3$-S catalysts.

increasing temperature. The maximum N_2O yields of 4, 20, 32, and 40% were obtained over $La_{0.8}Ce_{0.2}Cu_{0.4}Mn_{0.6}O_3$-R, $La_{0.8}Ce_{0.2}Cu_{0.4}Mn_{0.6}O_3$-S, $La_{0.8}Ce_{0.2}Ag_{0.4}Mn_{0.6}O_3$-R, and $La_{0.8}Ce_{0.2}Ag_{0.4}Mn_{0.6}O_3$-S, respectively. Therefore, the catalytic activity decreased in the order of $La_{0.8}Ce_{0.2}Cu_{0.4}Mn_{0.6}O_3$-R > $La_{0.8}Ce_{0.2}Cu_{0.4}Mn_{0.6}O_3$-S > $La_{0.8}Ce_{0.2}Ag_{0.4}Mn_{0.6}O_3$-R > $La_{0.8}Ce_{0.2}Ag_{0.4}Mn_{0.6}O_3$-S. It is concluded that perovskite-type oxides prepared by reverse microemulsion method showed much better catalytic performance (with higher NO conversion to N_2 and lower N_2O formation) than those synthesized by the sol–gel approach.

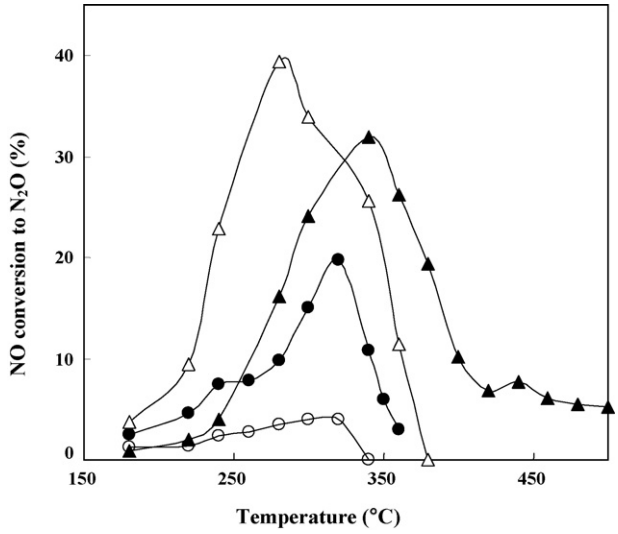

Fig. 2. NO conversion to N_2O over (○) $La_{0.8}Ce_{0.2}Cu_{0.4}Mn_{0.6}O_3$-R, (●) $La_{0.8}Ce_{0.2}Cu_{0.4}Mn_{0.6}O_3$-S, (△) $La_{0.8}Ce_{0.2}Ag_{0.4}Mn_{0.6}O_3$-S, and (▲) $La_{0.8}Ce_{0.2}Ag_{0.4}Mn_{0.6}O_3$-R catalysts for the reaction of NO and CO at SV = 20,000 h^{-1}.

3.2. Crystal structure and surface morphology

Fig. 3 shows the XRD results of $La_{0.8}Ce_{0.2}Cu_{0.4}Mn_{0.6}O_3$ and $La_{0.8}Ce_{0.2}Ag_{0.4}Mn_{0.6}O_3$. By comparing the XRD patterns with the ICDD PDF Database data of $LaMnO_3$ (No. 75-0440), one can realize that the main phase in the $La_{0.8}Ce_{0.2}Cu_{0.4}Mn_{0.6}O_3$ and $La_{0.8}Ce_{0.2}Ag_{0.4}Mn_{0.6}O_3$ was of rhombohedral perovskite-type structure. However, a considerable amount of CeO_2 was found in the samples synthesized via the sol–gel process. The intensities of diffraction peaks due to the CeO_2 phase were much lower in $La_{0.8}Ce_{0.2}Cu_{0.4}Mn_{0.6}O_3$-R and $La_{0.8}Ce_{0.2}Ag_{0.4}Mn_{0.6}O_3$-R than those in $La_{0.8}Ce_{0.2}Cu_{0.4}Mn_{0.6}O_3$-S and $La_{0.8}Ce_{0.2}Ag_{0.4}Mn_{0.6}O_3$-S, suggesting that the reverse microemulsion method favored the formation of perovskite structure and restrained the generation of CeO_2 phase. Fig. 4 exhibits TEM images of $La_{0.8}Ce_{0.2}Cu_{0.4}Mn_{0.6}O_3$. The $La_{0.8}Ce_{0.2}Cu_{0.4}Mn_{0.6}O_3$-S sample displayed particle aggregation of irregular shapes and in large size (Fig. 4a). However, the particles of the $La_{0.8}Ce_{0.2}Cu_{0.4}Mn_{0.6}O_3$-R sample were quite uniform and of spherical shape with a diameter of 40–50 nm (Fig. 4b). The surface areas of $La_{0.8}Ce_{0.2}Cu_{0.4}Mn_{0.6}O_3$-S, $La_{0.8}Ce_{0.2}Cu_{0.4}Mn_{0.6}O_3$-R, $La_{0.8}Ce_{0.2}Ag_{0.4}Mn_{0.6}O_3$-S, and $La_{0.8}Ce_{0.2}Ag_{0.4}Mn_{0.6}O_3$-R were 5.7, 14.2, 13.9, and 17.9 $m^2\ g^{-1}$, respectively. Compared with $La_{0.8}Ce_{0.2}Cu_{0.4}Mn_{0.6}O_3$ and $La_{0.8}Ce_{0.2}Ag_{0.4}Mn_{0.6}O_3$ derived with the sol–gel method, their counterparts prepared with the reverse microemulsion method possessed much higher surface areas, with an increase of 149 and 30%, respectively.

3.3. NO-TPD studies

In order to understand the reaction between NO and CO over the catalysts employed in this study, the adsorption and desorption of NO over the surface of $La_{0.8}Ce_{0.2}Cu_{0.4}Mn_{0.6}O_3$ and $La_{0.8}Ce_{0.2}Ag_{0.4}Mn_{0.6}O_3$ were investigated. Fig. 5 illus-

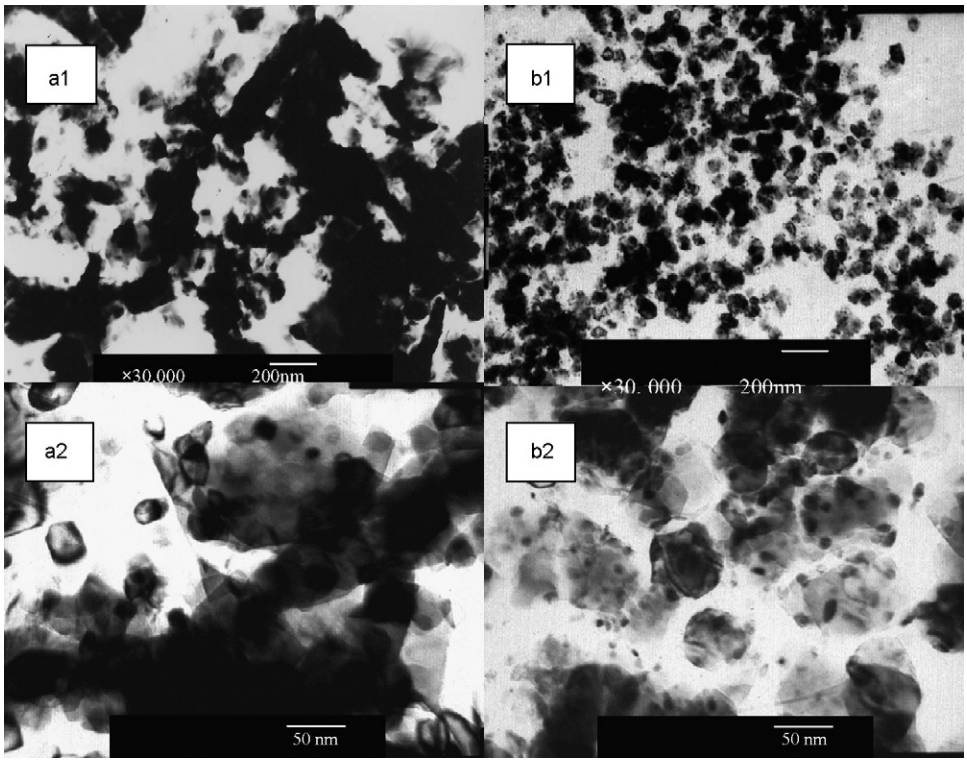

Fig. 4. TEM images of $La_{0.8}Ce_{0.2}Cu_{0.4}Mn_{0.6}O_3$-S (a) and $La_{0.8}Ce_{0.2}Cu_{0.4}Mn_{0.6}O_3$-R (b); a1 and b1: low-magnification images; a2 and b2: high-magnification images.

trates the NO-TPD profiles of $La_{0.8}Ce_{0.2}Cu_{0.4}Mn_{0.6}O_3$. Three NO desorption peaks at ca. 243, 322, and 415 °C over $La_{0.8}Ce_{0.2}Cu_{0.4}Mn_{0.6}O_3$-R and two peaks at ca. 243 and 415 °C over $La_{0.8}Ce_{0.2}Cu_{0.4}Mn_{0.6}O_3$-S were observed with a small peak of N_2O desorption at 223 and 324 °C over $La_{0.8}Ce_{0.2}Cu_{0.4}Mn_{0.6}O_3$-S and $La_{0.8}Ce_{0.2}Cu_{0.4}Mn_{0.6}O_3$-R, respectively. From Fig. 5, one can also see that the amount of NO adsorbed over $La_{0.8}Ce_{0.2}Cu_{0.4}Mn_{0.6}O_3$-R was larger than that over $La_{0.8}Ce_{0.2}Cu_{0.4}Mn_{0.6}O_3$-S. In the case of $La_{0.8}Ce_{0.2}Ag_{0.4}Mn_{0.6}O_3$ (Fig. 6), two NO desorption peaks at ca. 103 and 399 °C over $La_{0.8}Ce_{0.2}Ag_{0.4}Mn_{0.6}O_3$-R and those at ca. 103 and 395 °C over $La_{0.8}Ce_{0.2}Ag_{0.4}Mn_{0.6}O_3$-S were detected. The intensity of the first peak observed over $La_{0.8}Ce_{0.2}Ag_{0.4}Mn_{0.6}O_3$-R was much higher than that over $La_{0.8}Ce_{0.2}Ag_{0.4}Mn_{0.6}O_3$-S. For the two series of $La_{0.8}Ce_{0.2}Cu_{0.4}Mn_{0.6}O_3$ and $La_{0.8}Ce_{0.2}Ag_{0.4}Mn_{0.6}O_3$ catalysts, no matter what preparation method was employed, no significant desorption signals due to species of O_2, N_2, and NO_2 were detected during the NO-TPD process, indicating that the nondissociative adsorption of NO on the surfaces of the samples was dominant although a few of N_2O was generated via the following reactions [18]:

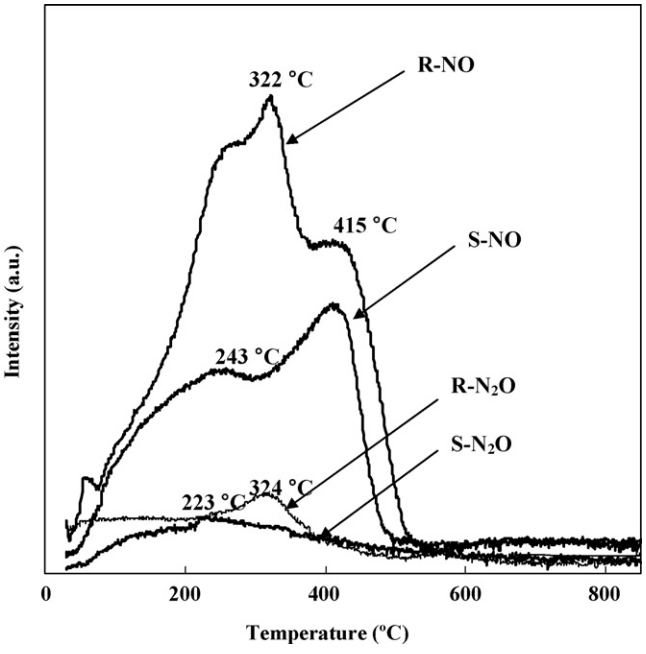

Fig. 5. NO-TPD profiles of $La_{0.8}Ce_{0.2}Cu_{0.4}Mn_{0.6}O_3$-R and $La_{0.8}Ce_{0.2}Cu_{0.4}Mn_{0.6}O_3$-S.

$$Cu-\square-Cu + NO \rightarrow Cu-O-Cu + N_{ads}$$

($\square$ represents a surface oxygen vacancy)

$$N_{ads} + NO \rightarrow N_2O$$

One should pay attention to that the small amount of N_2O could be found in the effluent in the NO-TPD experiments only over the $La_{0.8}Ce_{0.2}Cu_{0.4}Mn_{0.6}O_3$ catalyst, suggesting the Cu ions in the lattice of the perovskite-type oxide promoted the NO dissociative adsorption on the surface. The results show that the NO adsorption amount on perovskite-type oxides prepared by the reverse microemulsion method was more than that prepared via the sol–gel process, which was beneficial to the (NO + CO) reaction. Considering the difference in surface area, it is

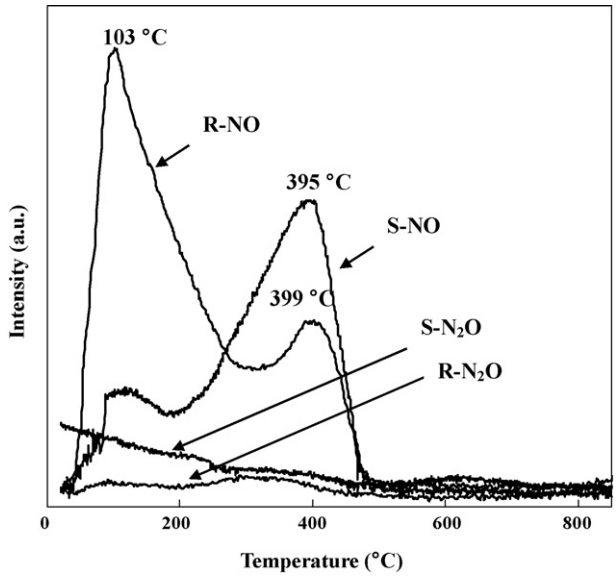

Fig. 6. NO-TPD profiles of $La_{0.8}Ce_{0.2}Ag_{0.4}Mn_{0.6}O_3$-R and $La_{0.8}Ce_{0.2}$-$Ag_{0.4}Mn_{0.6}O_3$-S.

understandable that the perovskite-type oxides prepared by the reverse microemulsion possess showed a large amount of NO adsorption.

3.4. XPS studies

Fig. 7 illustrates the Cu 2p spectra of $La_{0.8}Ce_{0.2}$-$Cu_{0.4}Mn_{0.6}O_3$-R and $La_{0.8}Ce_{0.2}Cu_{0.4}Mn_{0.6}O_3$-S. A relatively broad and asymmetric main Cu $2p_{3/2}$ line centered at 932.4 eV was observed, which could be assigned to the contribution of different copper species. According to the suggestion given by Terunuma [19], the binding energy (BE) of Cu $2p_{3/2}$ for Cu^0 and Cu^+ was ca. 932.5 eV, but Cu^{2+} shifted to higher BE by about 1.0 eV with a strong shake-up satellite structure at BE = 942.7 eV. From Fig. 7, it can be observed that the intensity of the shake-up satellite peak at BE = 942.7 eV was stronger and the peak centered at BE = 932.4 eV was broader for $La_{0.8}Ce_{0.2}Cu_{0.4}Mn_{0.6}O_3$-R than those for $La_{0.8}Ce_{0.2}$-$Cu_{0.4}Mn_{0.6}O_3$-S, implying that the Cu^{2+} content was higher in $La_{0.8}Ce_{0.2}Cu_{0.4}Mn_{0.6}O_3$-R.

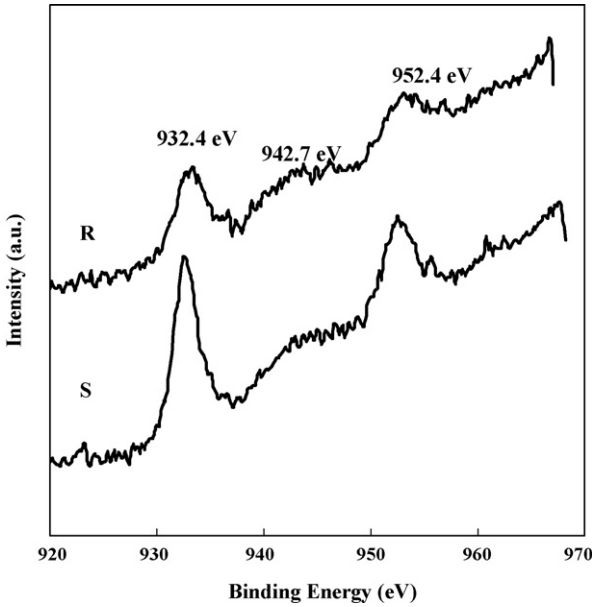

Fig. 7. Cu 2p spectra of $La_{0.8}Ce_{0.2}Cu_{0.4}Mn_{0.6}O_3$-R and $La_{0.8}Ce_{0.2}$-$Cu_{0.4}Mn_{0.6}O_3$-S catalysts.

4. Discussion

Perovskite-type oxides are promising materials as substitutes for precious metal catalysts in the removal of many pollutants, especially in the reaction of NO and CO. Generally speaking, the catalytic property of a perovskite-type oxide depends upon the nature of the B-site element and its structure defects, the latter can be regulated through the substitution of the A-site ion by other ions with a lower or higher oxidation state (e.g. Sr^{2+} or Ce^{4+}). Therefore, most of investigations were focused on the substitutions of both cationic sites. Such materials usually have small surface areas which do not favor the enhancement in catalytic activity. Recently, some studies on the preparation of the high-surface-area perovskite-type oxides have been reported [15]. In our present work, the $La_{0.8}Ce_{0.2}$-$Cu_{0.4}Mn_{0.6}O_3$-R and $La_{0.8}Ce_{0.2}Ag_{0.4}Mn_{0.6}O_3$-R catalysts prepared by reverse microemulsion method possessed high surface areas (14.2 and 17.9 $m^2\ g^{-1}$, respectively), and both of them exhibited the NO conversions considerably higher than those prepared by the sol–gel method.

The possible mechanism of nano-oxide formation in reverse microemulsion processes was proposed by Tai et al. [20]. After mixing both microemulsions containing the metal precursors, there was formation of primary particles whose sizes might be controlled by the reaction in the ‘‘nanoreactors’’ of the reverse microemulsion. The reaction was limited to the nanosized droplets distributed uniformly in the reverse microemuleion solution. Such a control would be beneficial for the formation of high-surface area uniform perovskite-type oxides. The images of TEM and surface areas of $La_{0.8}Ce_{0.2}Cu_{0.4}Mn_{0.6}O_3$ (R and S) and $La_{0.8}Ce_{0.2}Ag_{0.4}Mn_{0.6}O_3$ (R and S) confirm this deduction.

Teraoka et al. [21] reported that the NO can be adsorbed along with one oxygen atom and an electron flows to the NO molecule from a B-site cation, giving rise to the formation of the NO^- species. When particle size is reduced and surface area is increased, more surface defects and exposed B-site cation could be generated, thus the NO adsorption over the surfaces of perovskite-type oxides is enhanced. From Figs. 5 and 6, it can be realized that the $La_{0.8}Ce_{0.2}Cu_{0.4}Mn_{0.6}O_3$-R and $La_{0.8}Ce_{0.2}Ag_{0.4}Mn_{0.6}O_3$-R catalysts, which had small uniform particles and high surface areas, could adsorb more NO molecules than the $La_{0.8}Ce_{0.2}Cu_{0.4}Mn_{0.6}O_3$-S and $La_{0.8}Ce_{0.2}Ag_{0.4}Mn_{0.6}O_3$-S catalysts.

Leontiou et al. [11] summarized the previous works focused on the (NO + CO) reaction and proposed that this reaction proceeds via the three possible routes:

Route 1: $2NO + 2CO \rightarrow N_2 + 2CO_2$
Route 2: $2NO + CO \rightarrow N_2O + CO_2$
$N_2O \rightarrow N_2 + 1/2O_2$
Route 3: $NO \rightarrow N_2O + 1/2O_2$
$N_2O \rightarrow N_2 + 1/2O_2$

In the present experiments, N_2O was detected in the reaction system in the temperature range from 150 to 400 °C over our four catalysts. When the temperature was higher than 400 °C, no N_2O and O_2 molecules were measured in the reaction stream, which indicates that the Route 1 was dominated at high temperature, whereas at low reaction temperature the reaction between NO and CO proceeded possibly via the Routes 2 or 3 because a considerable amount of N_2O was detected. From Fig. 2, one can see that the concentration of N_2O measured in reaction effluent over the perovskite-type oxides prepared by the reverse microemulsion method was lower than that over the samples prepared by the sol–gel method, suggesting that the small particles of the perovskite-type oxides promoted the reaction of NO and CO via Route 1.

When NO molecules are adsorbed on the surface of the perovskite-type oxide, an electron flows to the NO molecule from a B-site cation to form the NO^- species, resulting in the concomitant oxidation of the B-site cation ($Cu^+ \rightarrow Cu^{2+}$, $Mn^{3+} \rightarrow Mn^{4+}$)[21]. The XPS results reveal that Ce^{4+} and Cu^+ (Fig. 7) were the predominant oxidation state for Ce and Cu components in $La_{0.8}Ce_{0.2}Cu_{0.4}Mn_{0.6}O_3$ and $La_{0.8}Ce_{0.2}Ag_{0.4}Mn_{0.6}O_3$. During the preparation process of the $La_{0.8}Ce_{0.2}Cu_{0.4}Mn_{0.6}O_3$ and $La_{0.8}Ce_{0.2}Ag_{0.4}Mn_{0.6}O_3$ catalysts, the following reaction

$$Ce^{3+} + Cu^{2+} \rightarrow Ce^{4+} + Cu^{+},$$

which accounts for the formation of Ce^{4+} and Cu^+ ions, would take place. The existence of Cu^+ and its redox action ($Cu^+ \leftrightarrow Cu^{2+}$) would facilitate the NO adsorption and reduction by CO. When the grain size of the perovskite-type catalyst reduced and the surface area increased, the more amount of Cu ions were exposed on the surface (which is beneficial to the redox process of $Cu^+ \leftrightarrow Cu^{2+}$), and then the catalytic activity for the reaction of NO and CO would be promoted. During the treatment of the catalysts in a flow of O_2, a part of Cu^+ would be oxidized to Cu^{2+}, resulting the enhancement of Cu^{2+} signal intensity in XPS spectra. The content of Cu^{2+} in $La_{0.8}Ce_{0.2}Cu_{0.4}Mn_{0.6}O_3$-R was higher than that in $La_{0.8}Ce_{0.2}Cu_{0.4}Mn_{0.6}O_3$-S as demonstrated in the XPS investigations, indicated the more Cu^+ ions on the surface were oxidized to Cu^{2+} and hence the former catalyst had better NO reduction activity than the latter.

5. Conclusions

$La_{0.8}Ce_{0.2}Cu_{0.4}Mn_{0.6}O_3$-R prepared by the reverse microemulsion method were uniform spherical nanoparticles with the diameter of 40–50 nm, whereas an agglomeration of particles was found for the $La_{0.8}Ce_{0.2}Cu_{0.4}Mn_{0.6}O_3$-S prepared by the sol–gel method. The surface areas of $La_{0.8}Ce_{0.2}Cu_{0.4}Mn_{0.6}O_3$-R (13.9 $m^2\ g^{-1}$) and $La_{0.8}Ce_{0.2}Ag_{0.4}Mn_{0.6}O_3$-R (17.9 $m^2\ g^{-1}$) obtained with the reverse microemulsion method increased 149 and 30%, respectively, in comparison with those of $La_{0.8}Ce_{0.2}Cu_{0.4}Mn_{0.6}O_3$-S (5.7 $m^2\ g^{-1}$) and $La_{0.8}Ce_{0.2}Ag_{0.4}Mn_{0.6}O_3$-S (14.2 $m^2\ g^{-1}$) obtained via the sol–gel approach. $La_{0.8}Ce_{0.2}Cu_{0.4}Mn_{0.6}O_3$-R showed high NO conversion at 20,000 h^{-1} and the NO/CO ratio = 1. The catalytic activity in the addressed reaction decreased in the order of $La_{0.8}Ce_{0.2}Cu_{0.4}Mn_{0.6}O_3$-R > $La_{0.8}Ce_{0.2}Cu_{0.4}Mn_{0.6}O_3$-S > $La_{0.8}Ce_{0.2}Ag_{0.4}Mn_{0.6}O_3$-R > $La_{0.8}Ce_{0.2}Ag_{0.4}Mn_{0.6}O_3$-S. The NO-TPD experiments showed that NO was the predominant desorbed species with a trace amount of O_2 and N_2O, suggesting that the nondissociative adsorption of NO on the surfaces of the perovskite-type oxides was dominant. The XPS results revealed that Ce^{4+} and Cu^+ were the predominant oxidation state for Ce and Cu components in $La_{0.8}Ce_{0.2}Cu_{0.4}Mn_{0.6}O_3$ and $La_{0.8}Ce_{0.2}Ag_{0.4}Mn_{0.6}O_3$ catalysts, respectively. The existence of Cu^+ and the redox action ($Cu^+ \leftrightarrow Cu^{2+}$) would beneficial to the adsorption of NO and hence to the reduction of NO by CO.

Acknowledgement

The work described in this paper was fully supported by the grants from (i) Beijing Municipal Commission of Education (Km200310005001) and (ii) Beijing Natural Science Foundation (3061001).

References

[1] V.C. Belessi, P.N. Trikalitis, A.K. Ladavos, T.V. Bakas, P.J. Pomonis, Appl. Catal. A 177 (1999) 53.
[2] N. Mizuno, M. Tanaka, M. Misono, J. Chem. Soc., Faraday Trans. 88 (1992) 91.
[3] A. Lindstedt, D. Strömberg, M. Abul Milh, Appl. Catal. A 116 (1994) 109.
[4] A. Kudo, M. Steinberg, A.J. Bard, A. Campion, M.A. Fox, T.E. Mallouk, S.E. Webber, J.M. White, J. Catal. 125 (1990) 565.
[5] M. Skoglundh, L. Löwendahl, K. Jansson, L. Dahl, M. Nygren, Appl. Catal. B 3 (1994) 259.
[6] L. Simonot, F. Garin, G. Maire, Appl. Catal. B 11 (1997) 181.
[7] Y. Teraoka, H. Nii, S. Kagawa, K. Jansson, M. Nygren, Appl. Catal. A 194–195 (2000) 35.
[8] M. Öcal, R. Oukaci, G. Marcelin, S.K. Agarwal, Ind. Eng. Chem. Res. 33 (1994) 2930.
[9] Y. Teraoka, H. Nii, S. Kagawa, K. Jansson, M. Nygren, J. Mater. Chem. 6 (1996) 97.
[10] S.T. Shen, H.S. Weng, Ind. Eng. Chem. Res. 37 (1998) 2654.
[11] A.A. Leontiou, A.K. Ladavos, P.J. Pomonis, Appl. Catal. A 241 (2003) 133.
[12] S.D. Peter1, E. Garbowski, V. Perrichon, B. Pommier, M. Primet, Appl. Catal. A 205 (2001) 147.
[13] V.C. Belessi, T.V. Bakas, C.N. Costa, A.M. Efstathiou, P.J. Pomonis, Appl. Catal. B 28 (2000) 13.
[14] V.C. Belessi, C.N. Costa, T.V. Bakas, T. Anastasiadou, P.J. Pomonis, A.M. Efstathiou, Catal. Today 59 (2000) 347.
[15] H. Tanaka, M. Misono, Curr. Opin. Solid State Mater. Sci. 5 (2001) 381.
[16] A.E. Giannakas, T.C. Vaimakis, A.K. Ladavos, P.N. Trikalitis, P.J. Pomonis, J. Colloid Interface Sci. 259 (2003) 244.
[17] Y. Sun, P.A. Sermon, J. Mater. Chem. 6 (1996) 1025.
[18] L. Forni, C. Olive, T. Barzetti, E. Sell, A.M. Ezerets, A.V. Vishniakov, Appl. Catal. B 13 (1997) 38.
[19] Y. Terunuma, K. Takahashi, T. Yoshizawa, Y. Momose, Appl. Surf. Sci. 115 (1997) 317.
[20] C.Y. Tai, M.-H. Lee, Y.-C. Wu, Chem. Eng. Sci. 56 (2001) 2389.
[21] Y. Teraoka, T. Harada, S. Kagawa, J. Chem. Soc. Faraday Trans. 94 (13) (1998) 1887.